AD NUMBER
AD915255
LIMITATION CHANGES

TO:

Approved for public release; distribution is unlimited.

FROM:

Distribution authorized to U.S. Gov't. agencies only; Test and Evaluation; 14 DEC 1973. Other requests shall be referred to Army Missile Command, Redstone Arsenal, AL 35809.
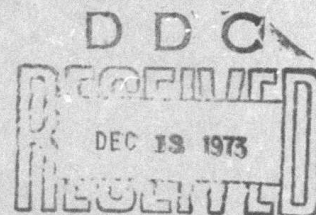
AUTHORITY

DARPA ltr, 17 Jun 1974

DENSITY AND TEMPERATURE DISTRIBUTIONS IN

HYPERSONIC CONE WAKES

J.G.G. Dionne and L. Tardif

CENTRE DE RECHERCHES POUR LA DEFENSE

DEFENCE RESEARCH ESTABLISHMENT

VALCARTIER

DEFENCE RESEARCH BOARD

CONSEIL DE RECHERCHES POUR LA DÉFENSE

Québec, Canada

August/août 1973

Statement B. T & E. per teleson with Mr. E.
Fronfield, Army Missile Command, attn:
AMSMI-BNS, Redstone Arsenal, Alabama 35809.

J. E. Cantt
14 Dec. 1973

DREV: R-695/73
PROJ: 95-51-10

DENSITY AND TEMPERATURE DISTRIBUTIONS IN HYPERSONIC CONE WAKES

by

J.G.G. Dionne — L. Tardif

Aug 73

28 p.

CENTRE DE RECHERCHES POUR LA DEFENSE

DEFENCE RESEARCH ESTABLISHMENT

VALCARTIER

Tel: (418) 844-4271

DN
404945

Québec, Canada

August/août 1973

RESUME

On a fait des mesures de la masse volumique dans le sillage de cônes hypersoniques en vol libre en utilisant une sonde à faisceau d'électrons. Les données recueillies ont permis de déterminer les distributions radiales et axiales de la masse volumique dans les sillages de cônes effilés de 44 et de 20° lancés à 15,500 pi/sec dans une atmosphère d'azote à 10 torr. On a mis à profit les mesures de la masse volumique pour inférer les distributions de température en supposant que le sillage est isobare et, qu'à une courte distance derrière le modèle, il obéit à la loi des gaz parfaits. (N C)

ABSTRACT

This report presents mass density measurements performed in the wake of hypersonic cones in free flight using the electron beam fluorescence probe technique. The radial and axial mass density distributions have been were obtained in the wake of sharp nose cones with vertex angles of 44 deg and 20 deg launched at 15,500 feet/second fps in a nitrogen atmosphere at 10 torr. The corresponding temperature distributions have been were inferred from the density data by assuming that the wake is isobaric and that the perfect gas law is valid a short distance behind the model.(U)

TABLE OF CONTENTS

1.0 INTRODUCTION

The experimental research program on hypersonic wakes undertaken in 1965 by the Defence Research Establishment Valcartier (DREV) in cooperation with the Advance Research Projects Agency (ARPA) of the United States has been oriented towards the collection of spatially resolved measurements of the fundamental observables of the flowfield. The wakes studied were generated in ballistic ranges by hypervelocity models, spheres and cones, launched by light gas guns in air and nitrogen atmospheres. The scope of the program has allowed the collection of data on the wakes of spheres with diameters varying from 0.4 to 2.7 inches and of cones with vertex angles of 44° and 20°. Mach numbers were varied from 3.5 to 13.5 and free stream Reynolds numbers from 3.3×10^4 to 1.0×10^6. The radial and axial distributions of velocity, mass density, temperature and charge density have been determined for several of these experimental conditions. The experimental techniques have been selected and developed to provide measurements with the best possible spatial and temporal resolutions.

To obtain mass density measurements in the wakes of hypersonic models, the electron beam fluorescence probe technique was selected and adapted to the ballistic range environment (Ref. 1). Mass density measurements performed with this technique in the wakes of hypersonic spheres have already been reported (Refs. 2 - 5).

To fulfill the objectives of the research program for mass density determination in hypersonic wakes, the final effort was devoted to data collection on cone wakes. The present report thus describes the mass density measurements performed in the wakes of sharp cones with 44° and 20° vertex angles. The wake temperature distributions inferred from the mass density data (assuming the wake is isobaric) are also reported. Special attention has been devoted to the particular problems that arise in the analysis of cone data. To assist the reader, a short summary of the experimental techniques and of the general analytical approach is given. For a more detailed description, the appropriate references are indicated in the text.

2.0 MASS DENSITY MEASUREMENT TECHNIQUE

The electron beam fluorescence probe used to measured mass density in the wake of hypersonic cones was adapted at DREV from the original concept proposed by Schumacher and Grün (Ref. 6) and developed by Muntz (Ref. 7). For operation in ballistic ranges, where moderately high pressures (1 to 10 torr) are necessary to generate turbulent wakes, two major limitations of the original technique had to be overcome: the strong departure from linearity shown by the fluorescent emission of the nitrogen gas molecule, and the rapid attenuation and severe spreading experienced by the beam in its path through the flowfield. These dif-

ficulties were alleviated by selecting the second positive band system of nitrogen $[N_2(2+)]$ at 3371 Å to reduce the non-linearity and by increasing the accelerating potential (from 30 kV to 100 kV) to reduce the attenuation and beam spreading. Nevertheless, the non-linearity and attenuation effects were taken into account in the data reduction scheme. In the worst case - largest pressure (10 torr) and largest distance between the measuring position and the electron beam origin (10 inches), - the correction factor did not exceed 12% for the non-linearity effect and 40% for the attenuation effect.

A detailed description of the electron beam fluorescence probe apparatus used at DREV has been given in Reference 1. Only a brief summary of the major characteristics will be presented here. The generator could produce a 1 to 2 mA beam current at an accelerating potential of 100 kV. A three stage differential pumping system allowed the operation of the electron gun chamber at 10^{-5} torr while a beam of 2 mm diameter was introduced into the ballistic range at pressures up to 10 torr. Three optical systems each incorporating four detectors collected the fluorescence emitted by the beam. The dimensions of each of the twelve fields of view were 1.2 x 12 mm. The amplified signals were displayed on oscilloscope screens and photographed with high speed Fastax cameras. A diagram of the experimental test section is shown in Figure 1.
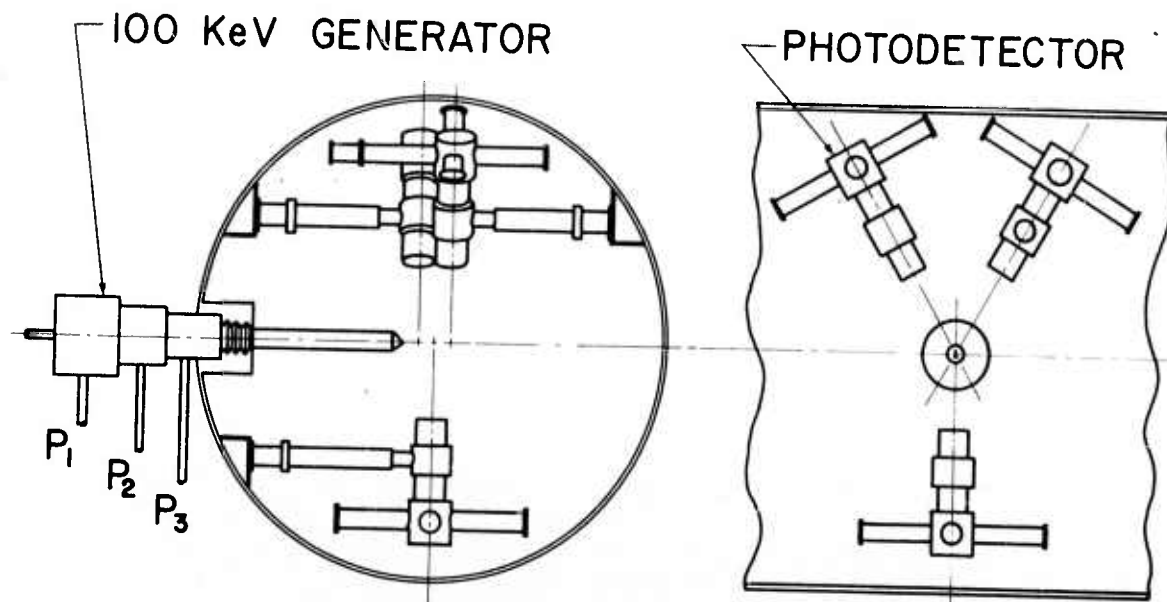

FIGURE 1 - Schematic of electron beam station for density measurements of cone wakes.

3.0 DATA ANALYSIS

The major problem in the analysis of the cone wake data arose from the difficulty of assessing the effects of the cone angle of attack. The angle of attack each cone had at the electron beam station was measurable but not predictable. Considering that the total number of firings was limited, it was not possible to obtain even a few launchings (3 to 5) with nearly identical angles of attack (less than 1° to 2° difference). Data from cones with different angles of attack had to be grouped to determine average mass density distributions. The following paragraphs describe the data analysis procedure developed to achieve this grouping.

3.1 Mass density data reduction

The raw signals obtained at each trial from the fluorescence detectors were processed in the same manner as were the signals from the density measurements in the wake of hypersonic spheres. The data reduction procedure has been described extensively in previous publications (Refs. 3 - 5). This process may be summarized as follows. The analog signal from each detector was digitized and converted from a recorded deflection to a local mass density ratio ρ/ρ_∞ (ρ_∞ = density outside the wake) by a computer program. The program took into account the various calibration parameters and the fluorescence-intensity-to-gas-density dependence. It also corrected for the effect of beam attenuation through an iteration procedure that took as a first density estimate the original signal from each detector. Thus, for each detector position, the mass density ratio was determined at each axial position behind the cone. The axial distance was measured in units of drag diameter, i.e. $\sqrt{C_D A}$, where C_D (drag coefficient) was evaluated for each cone depending on its angle of attack and A was the cone base area.

3.2 Determination of the angle of attack

To establish the cone trajectory and the flight attitude inside the aeroballistic range, X-ray stereophotography was used. The facility and technique have been reported elsewhere (Refs. 8 - 10). The measurements extracted from the X-ray photographs were analyzed with a digital computer to determine at several positions along the range both the flight path followed by the model center of gravity (C_g) and the attitude of the cone (pitch and yaw angles) at each of these positions. The model C_g position at the electron beam station was derived directly by interpolation along the flight path as the oscillations about a straight line were small. The cone attitude at the electron beam station was estimated by interpolation between the disdrete points of the pitch (θ) and yaw (ψ) angles measured at each photo-attitude station. However, because the oscillations of these values were large, the interpolation was done with the help of least-mean-square fits of the data using expressions of the form:
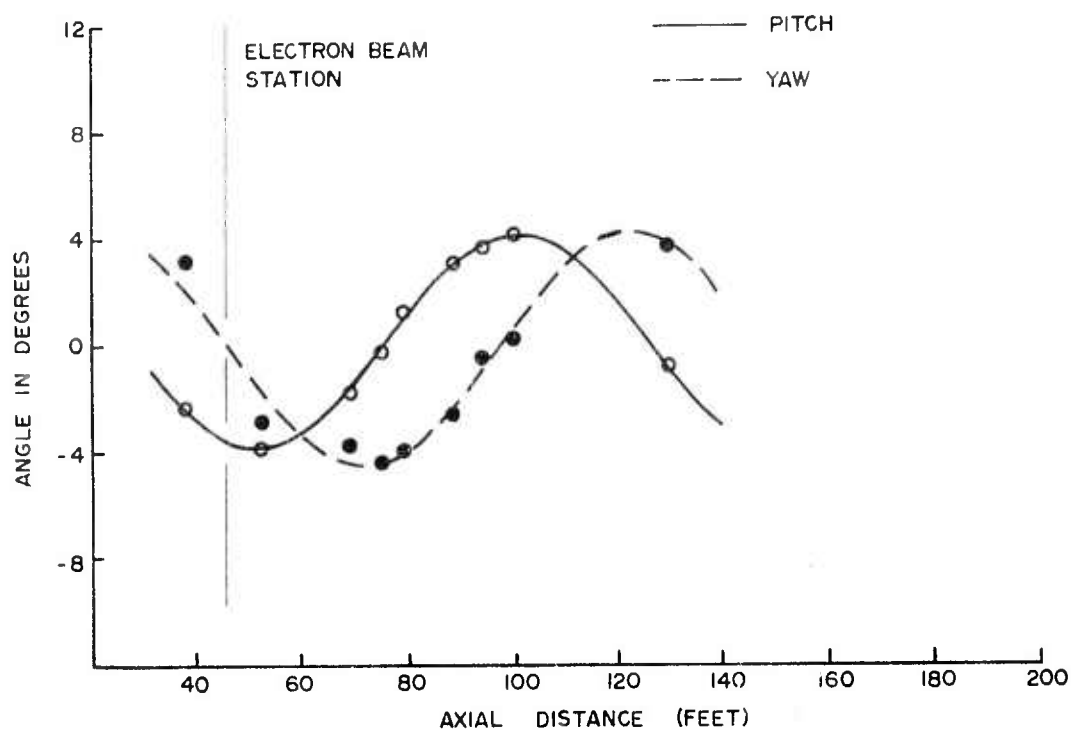
a) Typical pitch and yaw history for a 44° cone firing showing individual measurements and the L.M.S. fits.
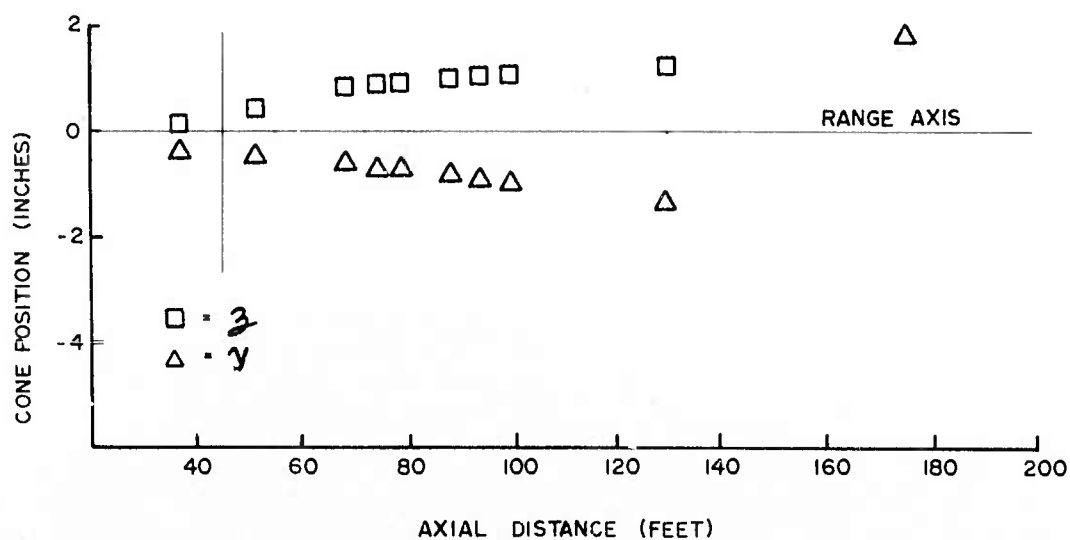
b) Trajectory of the cone C_g in the range.

FIGURE 2

$$\Theta(x) = \Theta_0 + \Theta_1 \sin(\frac{2\pi}{\lambda_\Theta} x + \phi_\Theta)$$

for the pitch angle where

$\Theta(x)$ is the pitch angle at position x behind the projectile

Θ_0 , the trim angle

Θ_1 , the amplitude of the oscillation

λ_Θ , the wavelength of the oscillation

ϕ_Θ , the phase angle of the oscillation with respect to the virtual origin.

For the yaw angle, the same expression was used except that Θ was replaced by ψ. The two wavelengths were assumed equal.

For each expression, the four parameters were fitted simultaneously. Typical results for a 44° cone firing are shown in Figure 2. For each firing, a set of such curves (pitch and yaw angles, C_g positions) were obtained.

From these curves, the position of each fluorescence detector for each firing was calculated with respect to the flight axis determined by the cone C_g and with respect to the cone pitch and yaw angles as shown in Figure 3.
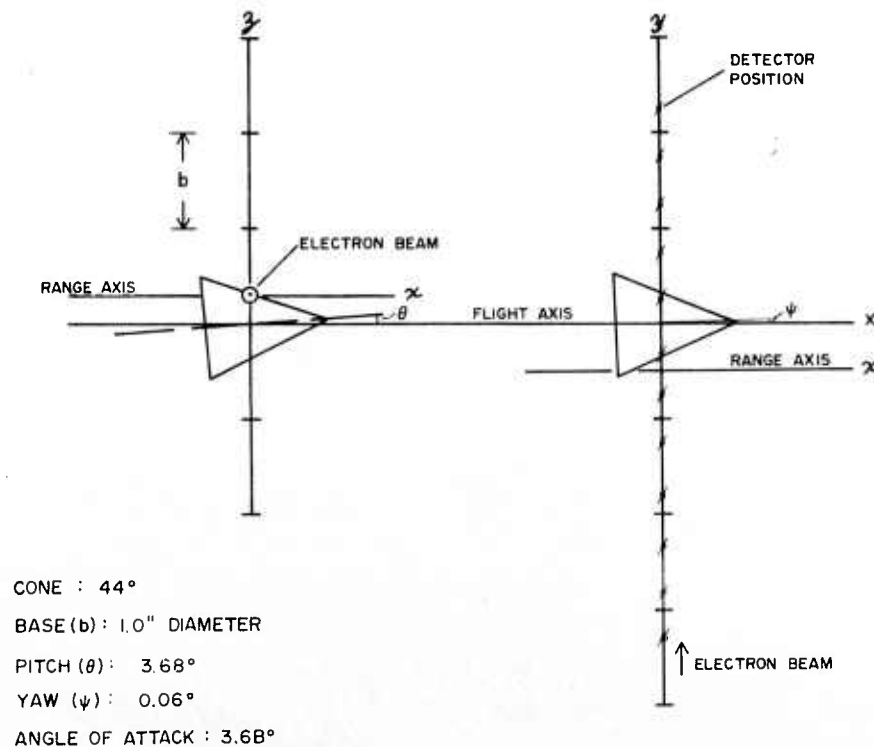

CONE : 44°

BASE (b) : 1.0" DIAMETER

PITCH (θ) : 3.68°

YAW (ψ) : 0.06°

ANGLE OF ATTACK : 3.68°

FIGURE 3 - Field of view positions of the fluorescence detector with respect to the cone attitude and position at the test section.
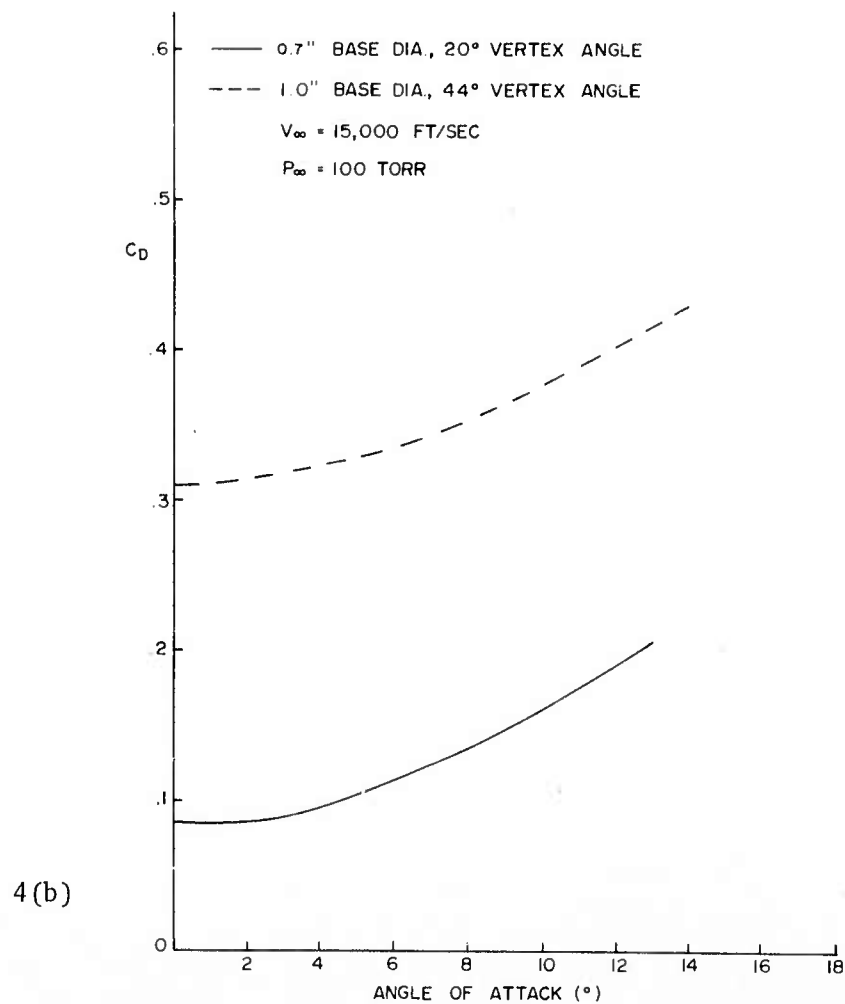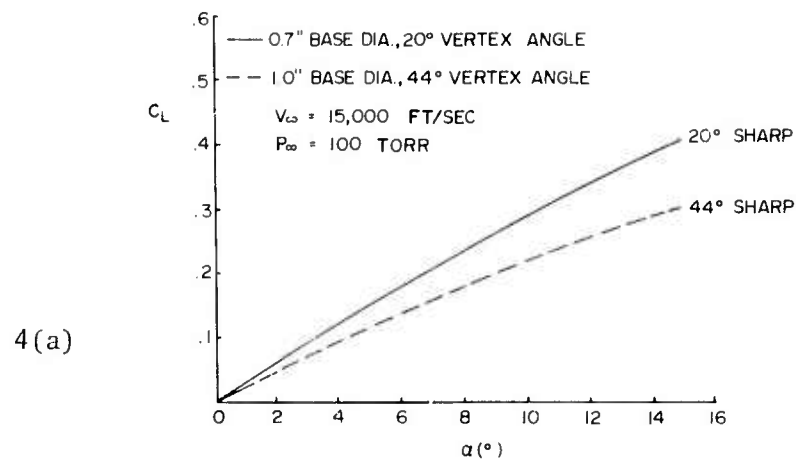
4(a)

4(b)

FIGURE 4 - Variation of the lift (a) and drag (b) coefficients with angle of attack for 20° and 44° vertex angle cones.

3.3 Drag and lift coefficients

Besides affecting the cone flight path, the angle of attack changes the amount of the energy lost due to drag. To compare cone firings with different angles of attack, it was necessary to evaluate the drag coefficient (C_D) for each firing.

The drag (C_D) and lift (C_L) coefficients were determined with the photoattitude X-rays and velocity stations on the ranges as reported by de Carufel et al. (Ref. 9) and Lahaye (Ref. 10). The cone drag and lift coefficients were obtained from Figure 4 for the angle of attack the cone exhibited when it passed the electron beam station.

3.4 Radial positions and wake deflection

Due to the large variations both in magnitude and direction of the cone angle of attack from firing to firing, it was necessary to establish the measurement positions in relation to a coordinate system defined by the cone attitude. To achieve this transformation the coordinate system had to be rotated about the wake axis to align different angles of attack in the same plane. The angle of rotation (β) was evaluated from the pitch and yaw angles at the electron beam station (x_{EB}) by the expression

$$\beta(x_{EB}) \ = \ \text{arc tan} \ \frac{\Theta(x_{EB})}{\psi(x_{EB})}$$

Once the rotation was performed the new position of each measuring volume was recalculated. The result of this transformation is equivalent to saying that, for all the cone firings, the angle of attack has always been in the same direction (but of different magnitude) and that the detector field of view positions were changed from firing to firing. Figure 5 illustrates this procedure.

Whenever a cone is flown at an angle of attack a vortex system is produced that induces a lateral displacement of the wake in the direction of the windward side of the cone. Using schlieren photographs, Lahaye (Ref. 10) has shown that, for 20° vertex angle cones, the wake deflection (δ) at various axial distances is independant of the angle of attack (α) when the deflection is normalized to the lift coefficient. Figure 6 presents the relation reported by Lahaye. The same author has also found that the 44° vertex angle cones do not show an appreciable wake deflection as the lift to drag ratio is small.

For the 20° vertex angle cones the wake deflection was evaluated at all positions behind the model. The position of each detector with respect to the wake axis was corrected by a translation along the Y axis in the rotated coordinate system equal in magnitude to the wake deflection shown in Figure 6, but in the direction opposite to the angle of attack. This is illustrated in Figure 7.
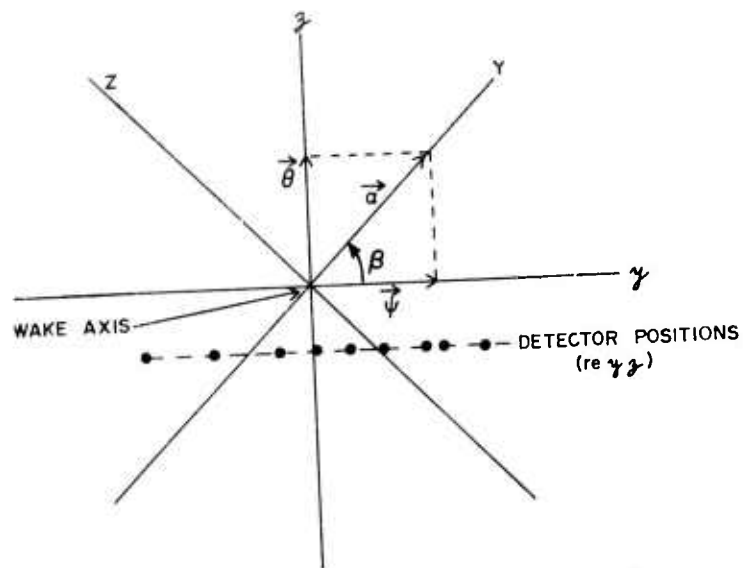
a) Field of view positions referenced to the flight coordinate systems (yz) and reference system (YZ) defined with respect to the angle of attack (α).
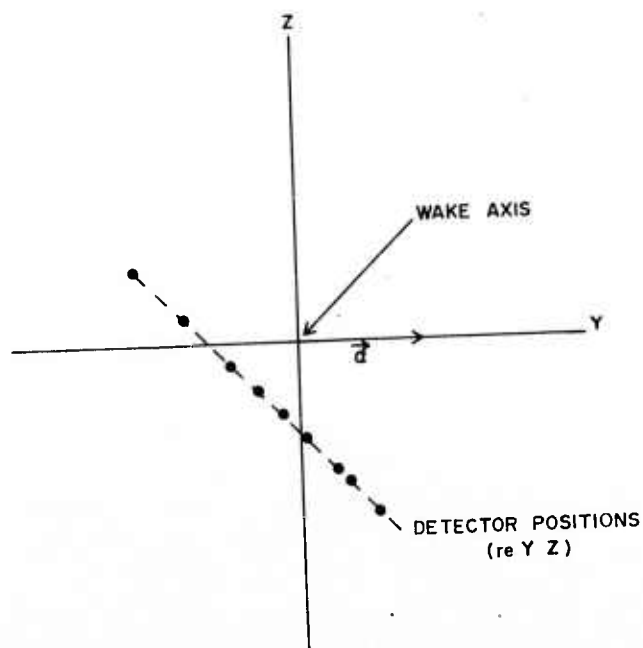
b) Field of view positions defined by alignment of the angle of attack on one axis.
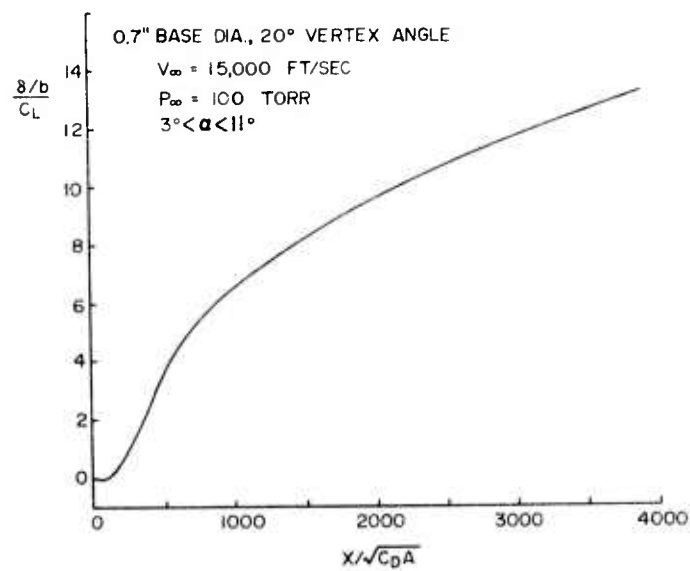
FIGURE 5

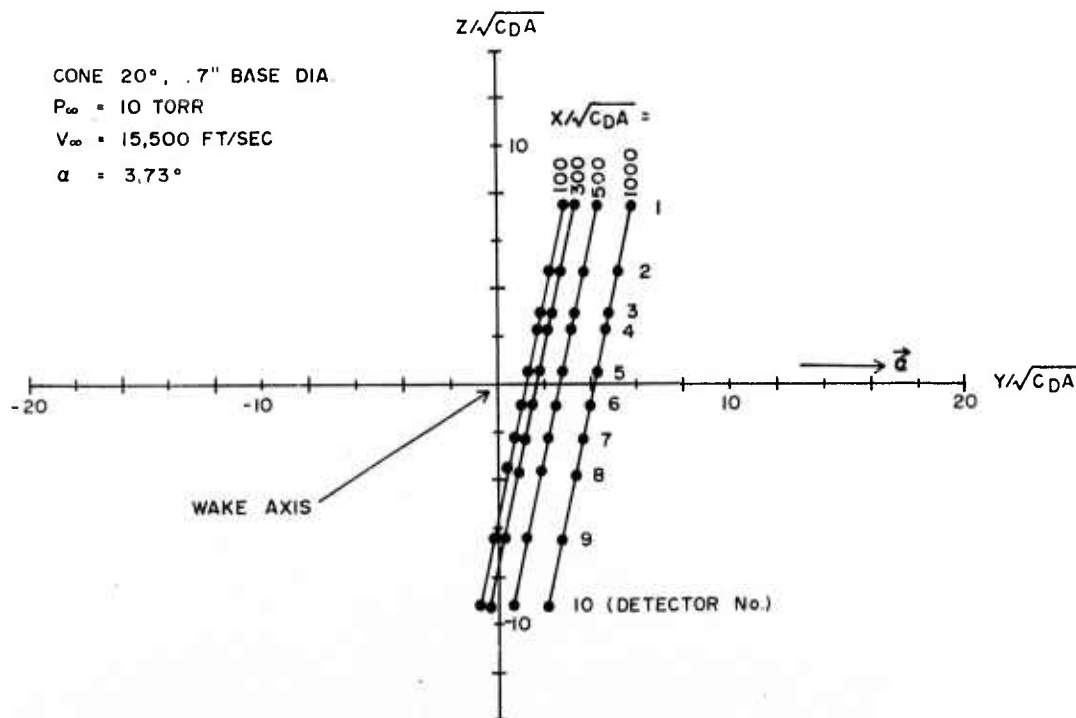FIGURE 6 - Variation of wake deflection with the axial distance.

FIGURE 7 - Effect of wake deflection on field of view positions.

3.5 Summary

The data reduction procedure for each firing may be summarized as follows.

a) The raw signals were processed using the same scheme as for sphere firings.

b) The coordinate system was translated from the range axis to the flight axis.

c) The coordinate system was rotated to bring the angle of attack into the designated quadrant of the XY plane.

d) The coordinate system was translated from the flight axis to the wake axis in the case of 20° cones, using a correction determined by the amplitude of the wake deflection.

4.0 EXPERIMENTAL MEASUREMENTS

The mass density measurements were performed in the DREV Range 3. The wakes were produced by sabot mounted cones launched at velocities of 15,500 feet/second in a nitrogen atmosphere at a pressure of 10 torr. Two cone models were used: a 44° vertex angle, 1.0 inch base diameter sharp nose cone and a 20° vertex angle, 0.7 inch base diameter sharp nose cone. Twelve 44° cone firings were included in the analysis with angles of attack varying from 0.9° to 18°, for a mean value of 9°. For the 20° cones, ten firings have been included with angles of attack varying from 1.3° to 7.3°, for a mean value of 4.7°.

It must be noted that measurements in the wake of 20° cones were particularly difficult. Firstly, the wake is geometrically small (about 1 to 2 inches), which implies that only a few detectors can take data at each firing; the detectors should not be positioned too close to each other as the exact flight line is not defined before firing. Secondly, the wake deflection is comparable to the wake diameter, so the wake moves rapidly out of the detector field of view for a deflection along the 'y' axis or it moves completely out of the field of view for a deflection along the 'z' axis. Thus the position of each measuring point with respect to the wake axis cannot be determined very accurately.

All cone firings with an angle of attack larger than the semi-vertex angle of the cone were rejected, because the measurements of drag coefficient and wake deflection used in the data analysis did not extend to such large angles of attack.

5.0 EXPERIMENTAL RESULTS

5.1 Radial distributions

To obtain a radial density distribution, the data from several firings are collected at a given axial position, $X/\sqrt{C_D A}$. However, because of the rotation and translation of the coordinate system, the radial positions at which measurements have been made are scattered over the whole YZ plane, i.e. the plane normal to the flight line.

The distribution of the points in the wake of the 44° cones where measurements were available is shown in Figure 8. Here the angles of attack are in the XY plane and in the positive direction of the Y axis. In the case of the 44° cones the radial distribution of the data measuring points remains the same at all axial positions since the wake deflection is too small to be measurable. For the 20° cones, the wake deflection varies with axial distance as shown in Figure 7. As the wake deflection also varies with angle of attack, the radial distribution of the measurement locations varies completely from one axial position to another. This variation is illustrated in Figure 9 where the distribution of data points at $X/\sqrt{C_D A} = 100$ (black dots) is compared to the distribution at $X/\sqrt{C_D A} = 500$ (open circles). The dashed lines point out the effects of wake deflection for some cases. The effect of the wake deflection is always in the same direction since all the angles of attack have been aligned in the XY plane along the Y axis as described before.

Using the density measurements corresponding to each datum point shown in Figure 8 for the 44° cones, an attempt was made to obtain a two dimensional density distribution by determining contours of constant density. Unfortunately the number of points available and their distribution in the YZ plane were not adequate to achieve this goal. Consequently, it was decided to reduce the problem to the determination of a one-dimension distribution by assuming the distribution to have an axis of symmetry. Since the angles of attack have been aligned in the XY plane along the Y axis, it was natural to assume that the distribution would be symmetrical about the Y axis and that the asymmetry induced by the angle of attack would appear about the Z axis.

Thus, for each point, a radial position $(R/\sqrt{C_D A})$ was computed with the expression $R = \pm \sqrt{Y^2 + Z^2}$. The radial value R was assigned the same sign as the value Y.

Under these assumptions the radial position of each datum point was calculated and the ensemble of results was used to obtain the radial mass density profiles at various axial positions. The density profiles for the 44° cones and the 20° cones are shown in Figures 10 and 11 respectively. Each point represents a mass density estimate (ρ/ρ_∞) obtained at a given radial position $(R/\sqrt{C_D A})$. The black squares represent the mean density values derived from ten consecutive points shown.

Consider the 44° cone profiles - the most striking feature is the asymmetry of the distribution in the direction opposite to the angle of attack. The position of minimum density on the graphs is shifted to the left by about 1 to 2 drag diameters; the density gradient is steeper on the left side and the density profile is skewed with respect to the flight line towards the windward side of the cone where the density gradient is steeper. The same description applies to all the profiles behind the 44° cones. In addition, as the axial distance increases, the profile widens and the scatter increases.

The 20° cone data, shown in Figure 11, have been analyzed in the same way as the 44° cone data. However, it was not possible to obtain data at an axial distance larger than 500 $X/\sqrt{C_D A}$ because the signal level became too small to be useful. The scatter in the data is such that the density profiles are not easily defined; however, some major features may be noted. Here again the wake has been shifted to the windward side of the cone and the overall density profile is relatively wide in drag diameter units. Moreover the large scatter in the data, even through the total number of firings is nearly as large as for the 44° cones, indicates that the use of wake deflection as a parameter is not sufficient to correlate wakes of cones with different angles of attack.

The radial profiles of the temperature excess shown in Figures 12 and 13 for the 44° and 20° cones respectively present the same general characteristics as the density profiles shown above. These temperature estimates have been inferred from the density data under the hypothesis that the perfect gas law is valid and the wake is isobaric a short distance behind the model. Once more the 20° cone wake appears larger in drag diameter units than the 44° cone wake. In both cases, the wake is shifted away from the flight line towards the windward side.

A comparison is presented in Figure 14 of the radial density profiles behind spheres and the two types of cones. The mass density defect normalized to the maximum value, $(1 - \rho_0/\rho_\infty)$, is plotted versus $R/\sqrt{C_D A}$. The solid line is derived from a least-mean-square fit of the mass density measurements obtained in the wake of spheres in the course of the same research program (Ref. 5). The 44° cone data, taken from Figure 10, show a wake width similar to the wake width for spheres but shifted by 1 to 2 drag diameters as mentioned earlier. The 20° cone data show a very wide wake in drag diameter units. This is surprising because width measurements have been made with schlieren photographs on the wakes of cones of the same dimensions (Ref. 10) and the results have shown that the wake width of cones is comparable to the wake width of spheres in drag diameter units. This discrepency in the 20° cone data may be attributed to the experimental difficulties experienced in the measurements behind 20° cones as mentioned earlier.
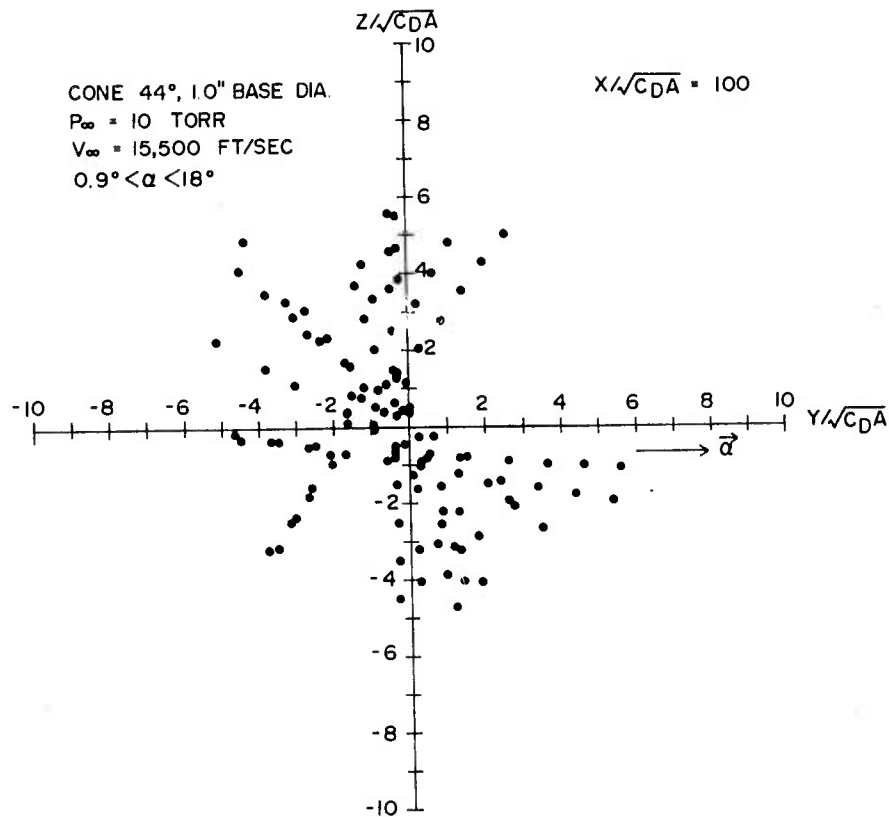
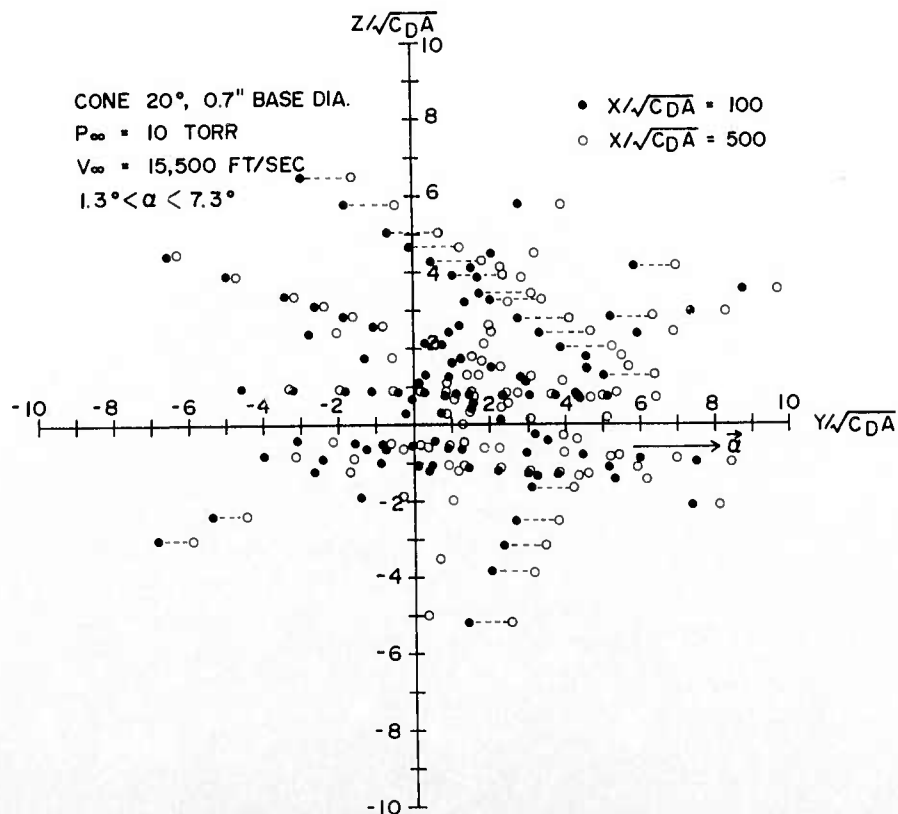FIGURE 8 - Radial distribution of measurement positions behind 44° cones.

FIGURE 9 - Comparison of radial distribution of measurement positions
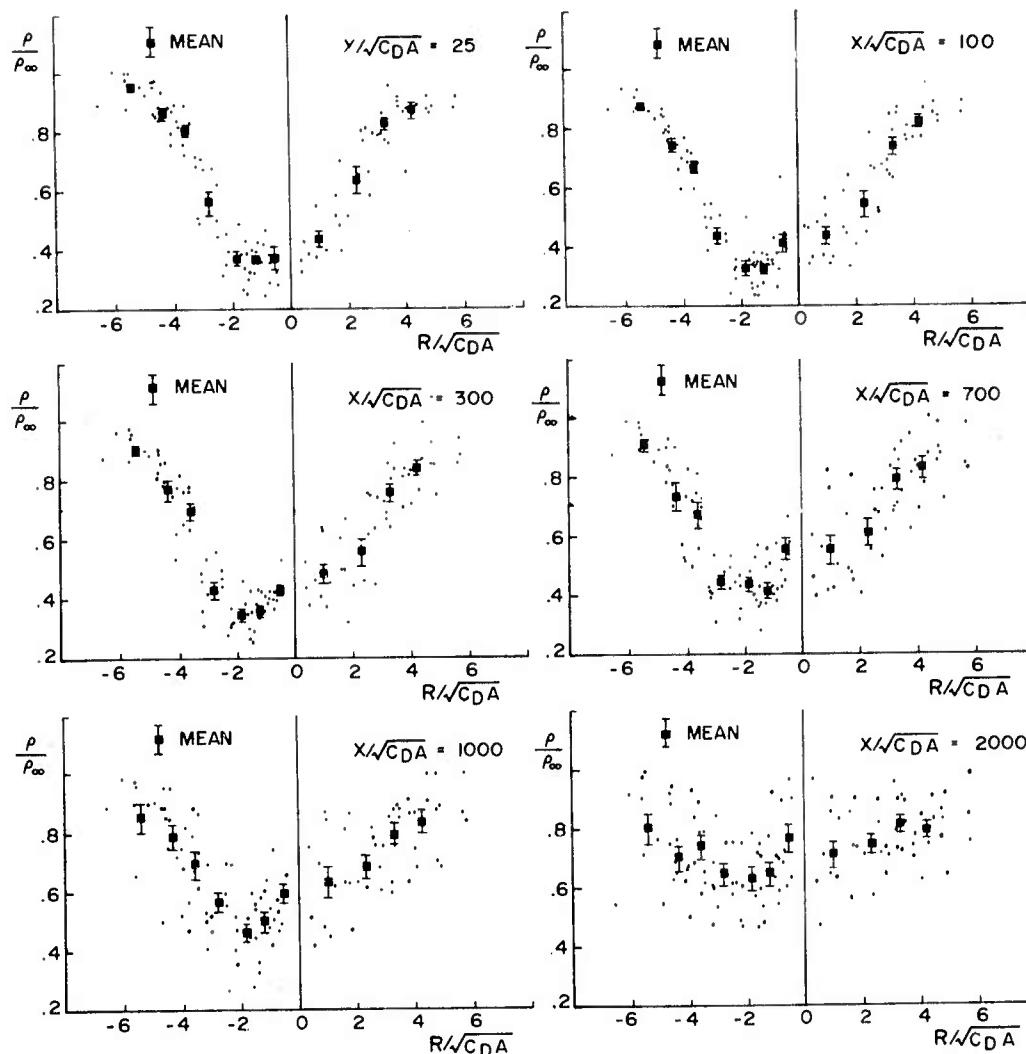behind 20° cones at two axial locations.

FIGURE 10 - Radial mass density profiles for 44° cones.

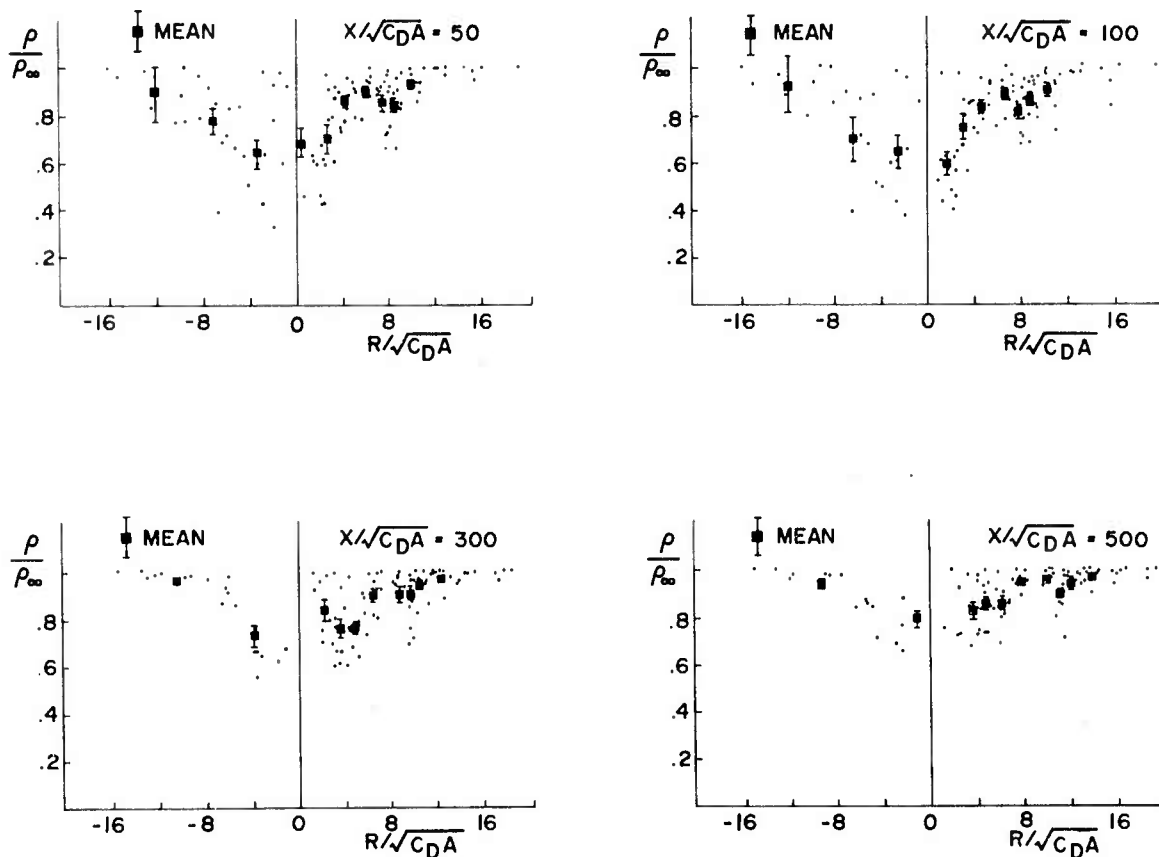CONE, 7" BASE; 20° INCLUDED ANGLE; 10 TORR; 15,500 FT/SEC
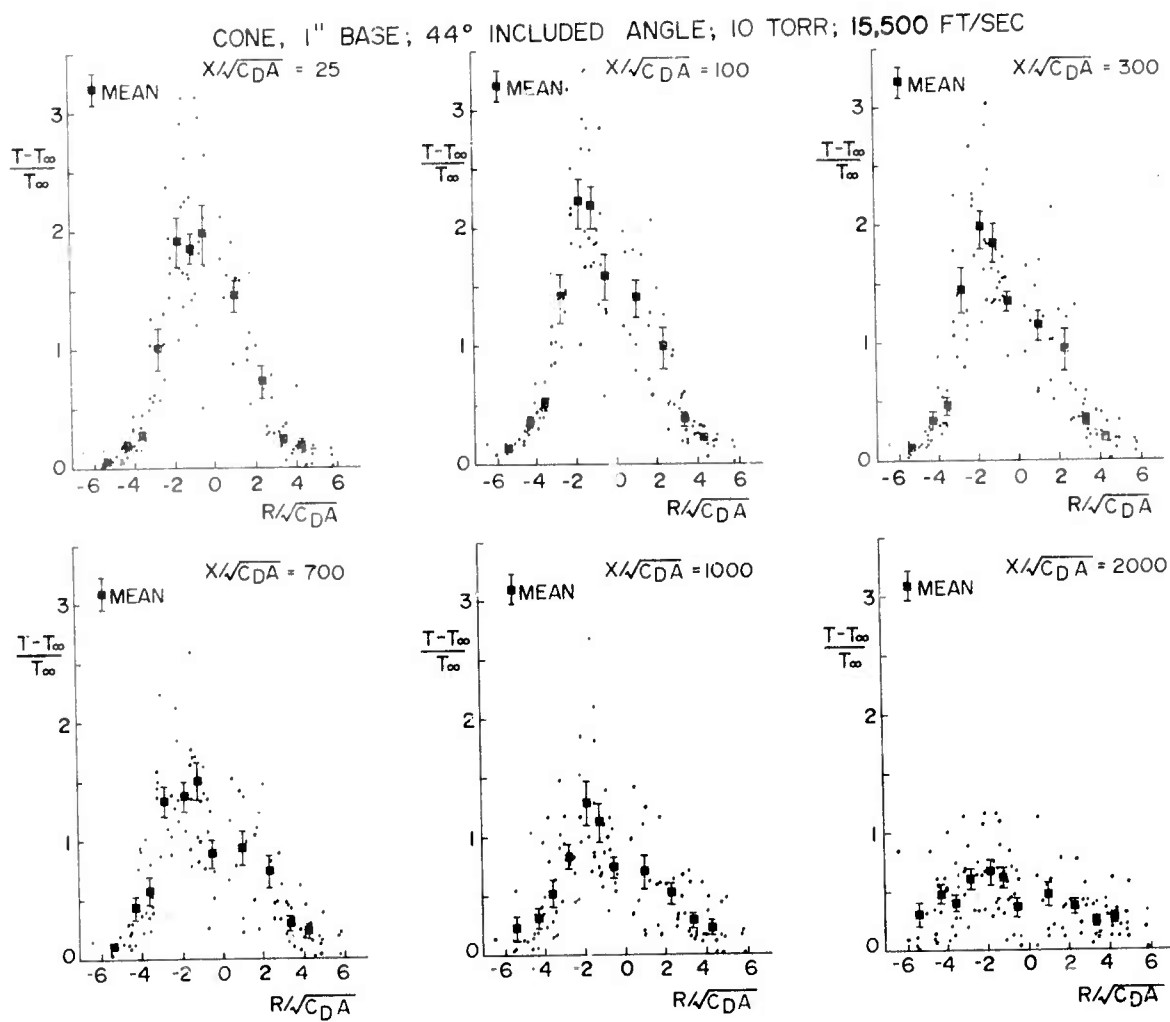

FIGURE 11 - Radial mass density profiles for 20° cones.

FIGURE 12 - Radial temperature excess profiles for 44° cones.
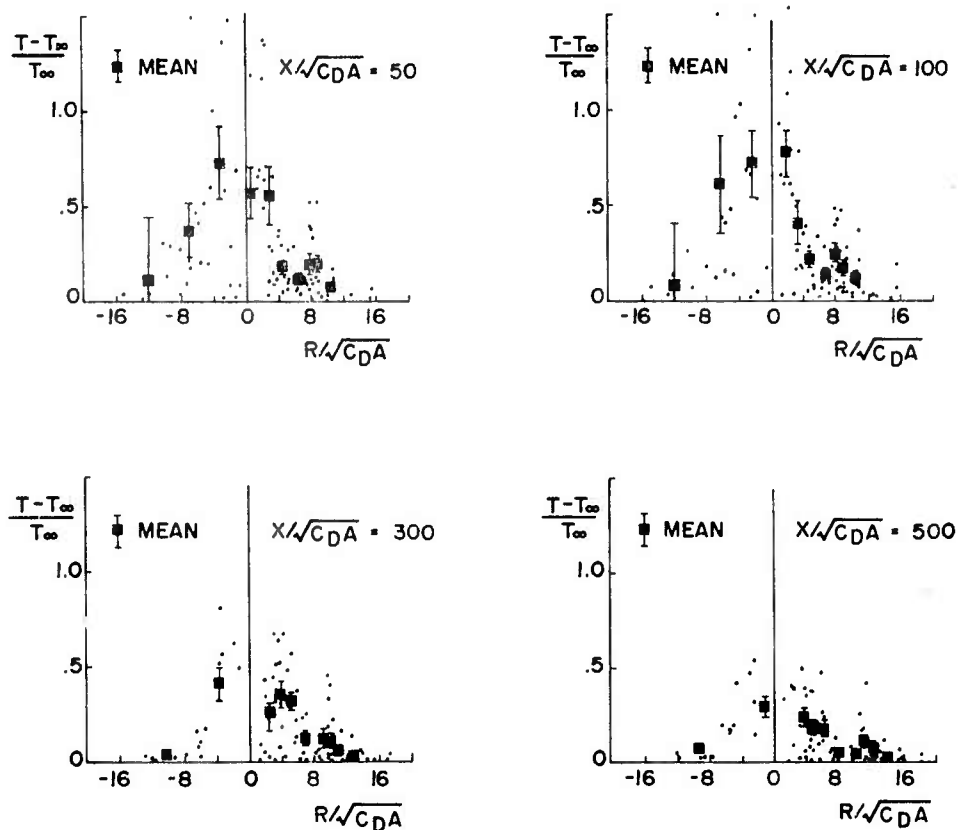
CONE, .7" BASE; 20° INCLUDED ANGLE; 10 TORR; 15,500 FT/SEC

FIGURE 13 - Radial temperature excess profiles for 20° cones.

—— SPHERE 1.0" DIA. (V_∞ = 15000 FT/SEC)

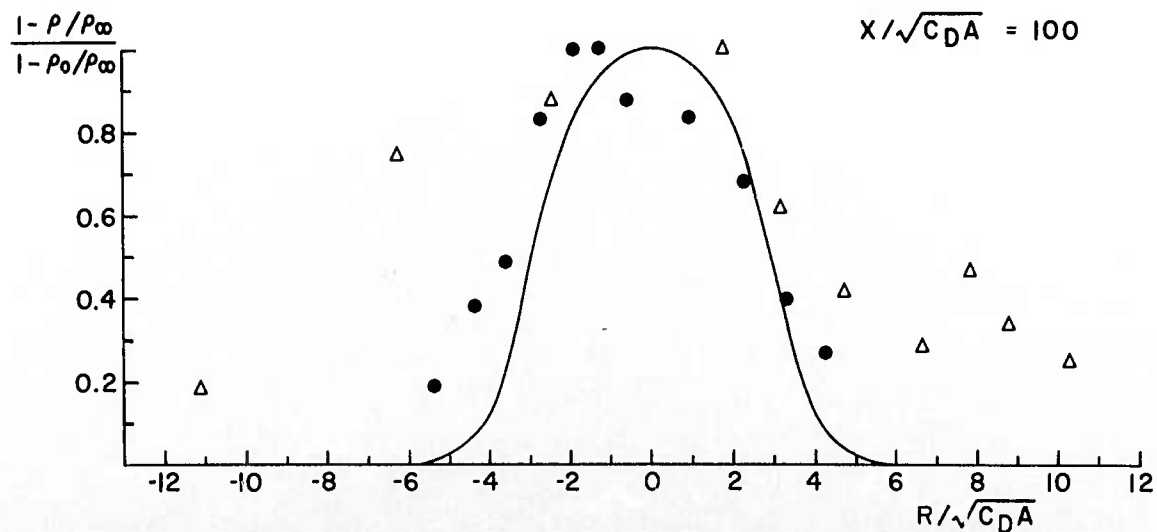● CONE 44° } V_∞ = 15,500 FT/SEC ρ_∞ = 10 TORR
△ CONE 20°

FIGURE 14 - Comparison of radial mass density defect for cones and spheres.

5.2 Axial distributions

Because of the large asymmetry in the radial profiles of the wakes of cones at angles of attack, it is difficult to determine the axial density distribution. With the data available for this study, the wake axis was defined as the position where the radial profile appeared to have a minimum for the mass density or a maximum for the temperature excess. In the case of the 44° cones, the wake axis appeared to be shifted between 1 and 2 drag diameters towards the windward side of the cone and the mean density ratio at $R/\sqrt{C} A = -1.2$ and -1.8 was used to derive the axial distribution of the mass density excess from the radial profile. An equivalent treatment was employed for the results with the 20° cones. However, because of the wake deflection effects, the geometrical distribution of points changed from profile to profile. From the radial profiles, there was no evidence that the wake axis changed position before 500 drag diameters. Therefore the mean density ratio corresponding to the radial position, $R/\sqrt{C} A = -3.3$, was selected. For several axial positions, it was necessary to perform a linear interpolation to obtain an estimate of the density at each radial position. From the density ratio, the density defect was evaluated at various axial distances. The same method was used to derive the axial variation of the temperature excess.

The axial distributions of the mass density defect behind spheres (Ref. 5) and 44° and 20° cones are compared in Figure 15. Up to 3000 drag diameters, the density defects for spheres and 44° cones show the same behavior, differing only by a constant factor. For the 20° cones, the density defect is much lower and its rapid decay begins earlier.

The comparison of the axial temperature excess for spheres and cones is shown in Figure 16. In the 44° cone wake, the temperature excess is smaller and its decay slower than is the case with sphere wakes up to 100 drag diameters. At higher axial distances, the temperature in the cone wake assumes the same rapid decay rate as in the sphere wake.

The 20° cone wake is still cooler than the 44° cone wake and it assumes a rapid decay rate earlier.
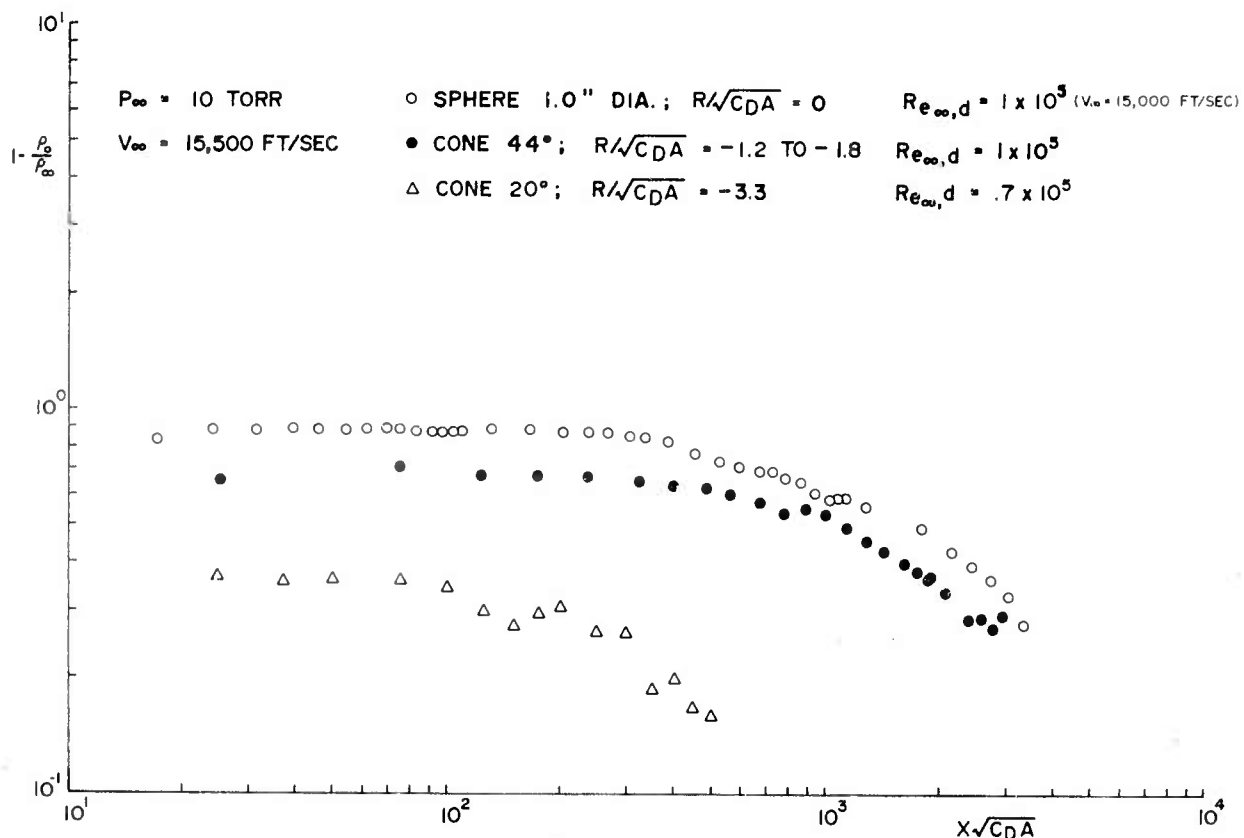
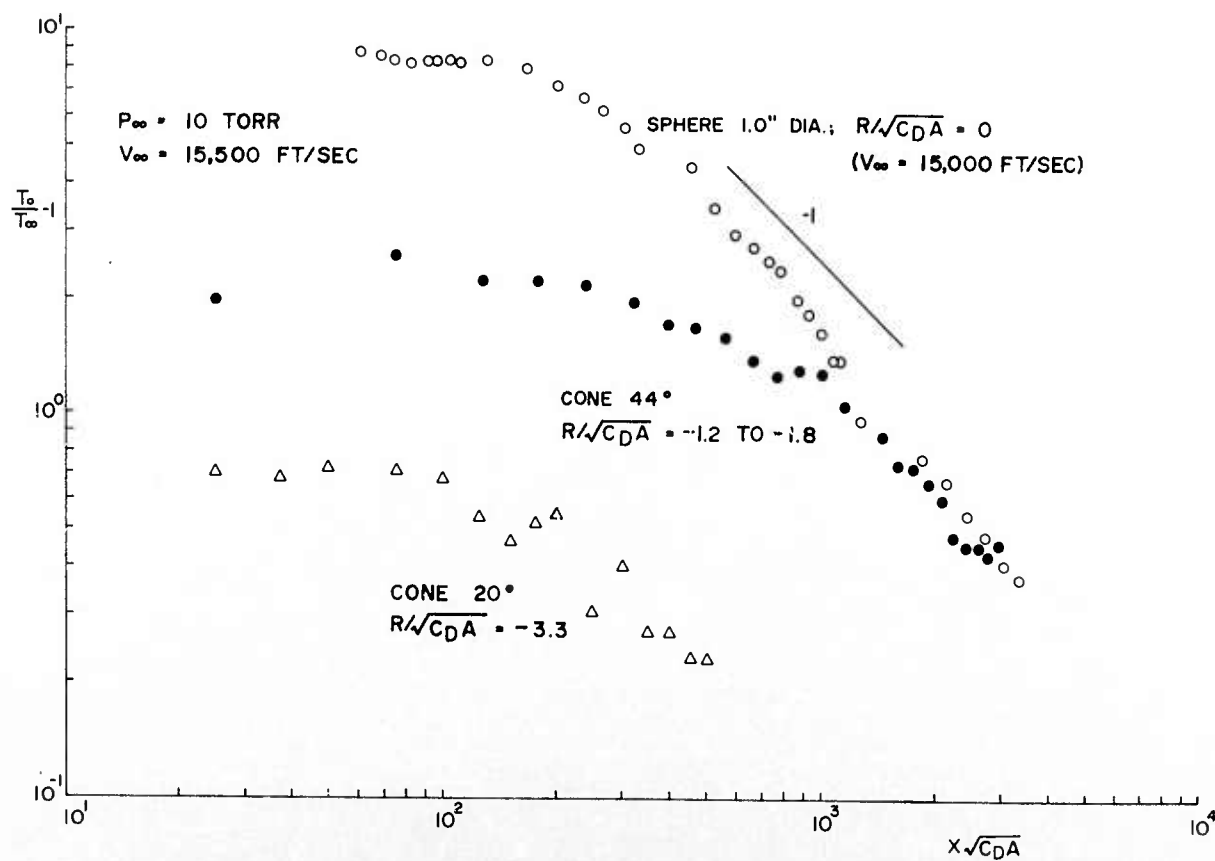FIGURE 15 - Centerline mass density defect for cones and spheres.

FIGURE 16 - Centerline temperature excess for cones and spheres.

6.0   CONCLUSIONS

The measurements reported here are quite unique in that the mass density data have been obtained at various positions in the wake of hypersonic sharp nose cones without interfering with the flowfield. It has been possible to perform these measurements across the whole width (even up to the axis) of the intermediate and far wake.

The results gathered from the wakes of cones flying at various angles of attack have been assembled in a common frame of reference by applying the appropriate geometrical transformation to the data from individual firings. Approximate radial distributions of mass density and temperature were derived from the resulting set of data points. This procedure has been particularly successful for the larger vertex angle cones (44°), but for the more slender cones (20°) the discrepencies in the radial profiles indicate that a more elaborate approach is needed to take into account the effects of the angle of attack on the flowfield.

The radial profiles and the axial variations of the mass density and temperature in the wakes of 44° vertex angle cones have been well established for small angles of attack. The radial density profiles show a large asymmetry induced by the cone angle of attack. However, because of the limited number of cone launchings available, it has not been possible to seek a relation between the amount of asymmetry and the angle of attack.

For the 20° cone wakes, because of the experimental and analytical problems caused by the angle of attack, the data collected do not indicate more than a very general feature, namely, the small amplitude and early decay of the axial distributions.

REFERENCES

1. Tardif, L. and Dionne, J.G.G., "Density Distribution in Turbulent and Laminar Wakes", AIAA Journal, Vol. 6, No. 10, pp. 2027-2029, October 1968.

2. Dionne, J.G.G. and Tardif, L., "Mean Density and Temperature Data in Wakes of Hypersonic Spheres", AIAA Journal, Vol. 8, No. 9, pp. 1707-1709, September 1970.

3. Dionne, J.G.G. and Tardif, L., "An Application of the Electron Beam Fluorescence Probe in Hyperballistic Range Wake Studies", ICIASF'71 Record, pp. 80-86, presented at the 4th International Congress on Instrumentation in Aerospace Simulation Facilities held at the Von Karman Institute for Fluid Dynamics, Rhode-Saint-Genèse, Belgium, 21-23 June 1971. (also DREV R 647/71).(Unclassified)

4. Dionne, J.G.G., Heckman, D., Lahaye, C., Sévigny, L. and Tardif, L., "Fluid Dynamic Properties of Turbulent Wakes of Hypersonic Spheres", AGARD Conference Proceedings No. 93 on Turbulent Shear Flows, (Fluid Dynamics Panel Specialists' Meeting, held in London, U.K., 13-15 September 1971). (also DREV R 654/72). (Unclassified)

5. Dionne, J.G.G. and Tardif, L., "Density and Temperature Distributions in Hypersonic Sphere Wakes", DREV R-683, September 72. (Unclassified).

6. Schumacher, B.W. and Grun, A.E. "Deutshe Patentanmeldung", Sch. 18144 IX 142-1, June 1955.

7. Muntz, E.P., "The Electron Beam Fluorescence Technique", AGARDograph 132, December 1968.

8. Léger, E.G. and Beaulieu, R., "Stereo Flash X-Ray Photoattitude Station for Use on Ballistic Ranges", CARDE T.R. 563/67. (Unclassified).

9. De Carufel, J., Lahaye, C. and Sévigny, L., "Etude du coefficient de traînée en fonction de l'angle d'attaque pour des cônes", DREV TN-1936/71, October 1971. (Unclassified).

10. Lahaye, C., "Experimental Study of Wakes Produced by Hypersonic Cone in Free Flight", DREV R-681, September 1972. (Unclassified).

DREV R-695/73 (UNCLASSIFIED)

CRDV, C.P. 880, Courcelette, Qué. - Conseil des recherches pour
la défense

"Density and Temperature Distributions in Hypersonic Cone Wakes"
J.G.G. Dionne et L. Tardif

On a fait des mesures de la masse volumique dans le sillage de
cônes hypersoniques en vol libre en utilisant une sonde à faisceau
d'électrons. Les données recueillies ont permis de déterminer les
distributions radiales et axiales de la masse volumique dans les sil-
lages de cônes effilés de 44 et de 20° lancés à 15,500 pi/sec dans
une atmosphère d'azote à 10 torr. On a mis à profit les mesures de
la masse volumique pour inférer les distributions de température en
supposant que le sillage est isobare et, qu'à une courte distance
derrière le modèle, il obéit à la loi des gaz parfaits. (N C)

DREV R-695/73 (UNCLASSIFIED)

CRDV, C.P. 880, Courcelette, Qué. - Conseil des recherches pour
la défense

"Density and Temperature Distributions in Hypersonic Cone Wakes"
J.G.G. Dionne et L. Tardif

On a fait des mesures de la masse volumique dans le sillage de
cônes hypersoniques en vol libre en utilisant une sonde à faisceau
d'électrons. Les données recueillies ont permis de déterminer les
distributions radiales et axiales de la masse volumique dans les sil-
lages de cônes effilés de 44 et de 20° lancés à 15,500 pi/sec dans
une atmosphère d'azote à 10 torr. On a mis à profit les mesures de
la masse volumique pour inférer les distributions de température en
supposant que le sillage est isobare et, qu'à une courte distance
derrière le modèle, il obéit à la loi des gaz parfaits. (N C)

DREV R-695/73 (UNCLASSIFIED)

CRDV, C.P. 880, Courcelette, Qué. - Conseil des recherches pour
la défense

"Density and Temperature Distributions in Hypersonic Cone Wakes"
J.G.G. Dionne et L. Tardif

On a fait des mesures de la masse volumique dans le sillage de
cônes hypersoniques en vol libre en utilisant une sonde à faisceau
d'électrons. Les données recueillies ont permis de déterminer les
distributions radiales et axiales de la masse volumique dans les sil-
lages de cônes effilés de 44 et de 20° lancés à 15,500 pi/sec dans
une atmosphère d'azote à 10 torr. On a mis à profit les mesures de
la masse volumique pour inférer les distributions de température en
supposant que le sillage est isobare et, qu'à une courte distance
derrière le modèle, il obéit à la loi des gaz parfaits. (N C)

DREV R-695/73 (UNCLASSIFIED)

CRDV, C.P. 880, Courcelette, Qué. - Conseil des recherches pour
la défense

"Density and Temperature Distributions in Hypersonic Cone Wakes"
J.G.G. Dionne et L. Tardif

On a fait des mesures de la masse volumique dans le sillage de
cônes hypersoniques en vol libre en utilisant une sonde à faisceau
d'électrons. Les données recueillies ont permis de déterminer les
distributions radiales et axiales de la masse volumique dans les sil-
lages de cônes effilés de 44 et de 20° lancés à 15,500 pi/sec dans
une atmosphère d'azote à 10 torr. On a mis à profit les mesures de
la masse volumique pour inférer les distributions de température en
supposant que le sillage est isobare et, qu'à une courte distance
derrière le modèle, il obéit à la loi des gaz parfaits. (N C)

DREV R-695/73 (UNCLASSIFIED)

DREV, P.O. Box 880, Courcelette, Qué. - Defence Research Board
of Canada

"Density and Temperature Distributions in Hypersonic Cone Wakes"
J.G.G. Dionne and L. Tardif

This report presents mass density measurements performed in the wake of hypersonic cones in free flight using the electron beam fluorescence probe technique. The radial and axial mass density distributions have been obtained in the wake of sharp nose cones with vertex angles of 44° and 20° launched at 15,500 feet/second in a nitrogen atmosphere at 10 torr. The corresponding temperature distributions have been inferred from the density data by assuming that the wake is isobaric and that the perfect gas law is valid a short distance behind the model. (U)

DREV R-695/73 (UNCLASSIFIED)

DREV, P.O. Box 880, Courcelette, Qué. - Defence Research Board
of Canada

"Density and Temperature Distributions in Hypersonic Cone Wakes"
J.G.G. Dionne and L. Tardif

This report presents mass density measurements performed in the wake of hypersonic cones in free flight using the electron beam fluorescence probe technique. The radial and axial mass density distributions have been obtained in the wake of sharp nose cones with vertex angles of 44° and 20° launched at 15,500 feet/second in a nitrogen atmosphere at 10 torr. The corresponding temperature distributions have been inferred from the density data by assuming that the wake is isobaric and that the perfect gas law is valid a short distance behind the model. (U)